

# Two-phase flow component fraction measurement using gamma-ray attenuation technique

Mohsen Sharifzadeh<sup>1,3</sup> · Hosein Khalafi<sup>2</sup> · Hosein Afarideh<sup>3</sup> · Ehsanallah Noori<sup>4</sup>

Received: 19 September 2016/Revised: 23 October 2016/Accepted: 25 January 2017/Published online: 25 May 2017  
© Shanghai Institute of Applied Physics, Chinese Academy of Sciences, Chinese Nuclear Society, Science Press China and Springer Science+Business Media Singapore 2017

**Abstract** Multiphase flow meters as the potential alternatives to separation and metering techniques have been in rapid development since 1980s. Before its field operation, the instrument should be calibrated in a standard test-facility. In spite of the known medium and large scale facilities all over the world, we developed a laboratory scale instrument for component fraction measurements. It has a two-phase flow homogenizer loop with the clamp-on potential of the meters to provide a regime independent measurement. It is capable of delivering a complete homogenization by  $\gamma$ -ray densitometer. With an error of  $\pm 5\%$  in component fraction measurements, this instrument is appropriate for testing and calibrating other meters.

**Keywords** Component fraction measurement · Homogenization · MATLAB-Based algorithm · Pencil-beam collimation · Gamma-ray attenuation

---

The work has been financially supported by Radiation Application Research School as a part of Nuclear Science and Technology Research Institute.

---

✉ Mohsen Sharifzadeh  
mssharifzadeh@aeoi.org.ir

<sup>1</sup> Radiation Application Research School, Nuclear Science and Technology Research Institute, Tehran 14399-51113, Iran

<sup>2</sup> Nuclear Science and Technology Research Institute, Tehran 14399-51113, Iran

<sup>3</sup> Department of Energy Engineering and Physics, AmirKabir University of Technology, Tehran 15875-4413, Iran

<sup>4</sup> Plasma Research School, Nuclear Science and Technology Research Institute, Tehran 14399-51113, Iran

## 1 Introduction

In a petroleum pipeline, multiphase flow (oil–gas–water mixtures) obviously shows off, and the problem of how to accurately measure the flow rate remains a challenge in the petroleum industry [1]. As proposed by the American Petroleum Institute [2] and the Norwegian Society for Oil and Gas Measurement [3], one strategy is to separate the flow into liquid (oil plus water) and gas streams and measure them using either traditional three-phase flow meters, or two- and single-phase flow meters. Homogenizing the flow can reduce difficulties in measuring the multiphase flow rate.

Before its operation in specific conditions in the field, a multiphase flow meter should be calibrated in a standard test-facility. Typical test facilities include three-phase flow loop at the Christian Michelsen Research Center [4], dual sets of high-pressure and low-pressure flow loops at the Pro-Lab National Laboratory [5], the flow component testing facilities at the Southwest Research Institute [6], and so on. Along with the studies began recently on multiphase flow meters at the Radiation Application Research School as a part of Nuclear Science and Technology Research Institute in Tehran, it seemed essential to design a new laboratory scale test-facility to test and calibrate multiphase flow meters. It is a two-phase flow homogenizer loop with the clamp-on potential of the meters to provide a regime independent condition for component fraction measurements.

This paper, as a part of the first author's PhD thesis, presents the results in a feasibility study to design and construct a homogenizer loop with a pre-verified gamma-ray densitometer to measure the component fraction of two-phase (solid–liquid) mixtures. The verified loop will

be used for oil–water two-phase fraction measurements. In future, by adding a bubble generation mechanism, it will be converted to a three-phase flow homogenizer loop for oil–gas–water fraction measurements by using a dual-energy gamma attenuation technique.

## 2 The problem

As known, the mass and volumetric flow rates of the phases are the main information used to characterize a multiphase flow. The mass flow rate of a multiphase flow is given by

$$M = A \sum_i \rho_i \alpha_i v_i, \tag{1}$$

where  $A$  is the pipe cross-section; and  $\rho_i$ ,  $\alpha_i$  and  $v_i$  are the density, component fraction and velocity of the individual phases, respectively. Figure 1 shows the inferential method for oil–gas–water three-phase flow measurement. However, the component fraction module remains an important field of study and needs a test-facility for calibrating the instruments developed.

### 2.1 Homogenization strategy

In order to overcome the problem of regime dependent for component fraction measurements, four methods are used commonly: (1) multi-beam gamma-ray densitometry [8–10]; (2) flow imaging tomographic systems [11, 12]; (3) dual modality technique, including transmitted and scattered gamma-ray counting [13–15] and using artificial neural network as a pattern recognition technique [16]; and (4) using a homogenization mechanism to remove all of the possible regimes [17]. Flow homogenization before measurement, is an elegant strategy, which causes the mixture density to be the same across the pipe cross section, and therefore reduces the number and difficulty of

measurements required. Homogenization simplifies the flow rate measurements, and reduces the slip between the phases. It makes individual phases have the same velocity, removes all the possible flow regimes except homogenous one, and makes a regime independent component fraction measurement.

### 2.2 Gamma-ray densitometry

Gamma-ray attenuation obeys the Lambert–Beer’s exponential decay law

$$I = I_0 B \exp\left(-d \sum_i \alpha_i \mu_i\right), \tag{2}$$

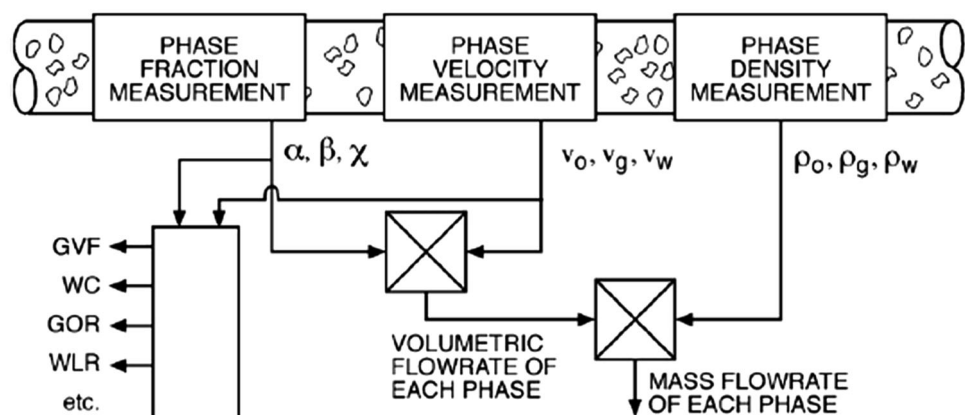
where  $I$  is the measured intensity;  $I_0$  is the initial intensity;  $\alpha_i$  and  $\mu_i$  are the component fraction and linear attenuation coefficient of individual phases, respectively;  $d$  is the effective inner diameter of the pipe; and  $B$  is the buildup factor due to scattered radiation. Assuming that the pipe is filled with a two-phase mixture and  $B = 1$ , by the establishment of the good geometry conditions, the component fractions can be extracted as

$$\begin{cases} \alpha_i = \ln(I_2/I_{mix})/\ln(I_2/I_1) \\ \alpha_2 = 1 - \alpha_1 \end{cases}, \tag{3}$$

where  $\alpha_1$  and  $\alpha_2$  are the dispersed and carrier phase fractions, respectively;  $I_{mix}$  is the mixture count rate; and  $I_1$  and  $I_2$  are the count rates relating to the calibration stage, with the pipe being fully filled by the dispersed and carrier phases at each time. While working with a suspension, it is impossible to fill the loop by the solid (dispersed) phase entirely. Thus, one can consider a maximum permissible fraction of  $t \leq 1$ . In this case, the component fractions can be calculated by

$$\begin{cases} \alpha_i = t \times (\ln(I_2/I_{mix})/\ln(I_2/I_1)) \\ \alpha_2 = 1 - \alpha_1 \end{cases}. \tag{4}$$

**Fig. 1** The inferential approach to the three-phase flow measurement problem [7]



### 3 The TPFHL (two phase flow homogenizer loop) project

The aim is to develop a homogenizer loop with  $\gamma$ -ray attenuation technique to measure two-phase component fractions (Fig. 2).

#### 3.1 Mechanical design

##### 3.1.1 Homogenization tank

For converting a suspension to a homogenized mixture, calculations were done on various kinds of parameters of the homogenization tank, and finally we used a 4" diameter (a common oil pipe diameter) cylindrical tank with dished bottom to maximize suspension quality, in height of 60 cm, enough for placing the meters. On the tank wall, there were two Plexiglas windows opposite to each other, used as a material of low  $\gamma$ -ray attenuation coefficient and to make more accurate measurements by reducing the statistical errors. Sixteen 45° pitched blade turbine (PBT) type impellers were used, each consisting of four flat blades of 1 cm width and 2 mm thickness.

According to the standard handbook of industrial mixing [18], the best compromise between shearing and flow pumping was decided to achieve complete homogenization. In order to deliver a uniform suspension, which means practically uniform in particle concentration and size



**Fig. 2** (Color online) The TPFHL test-facility. A homogenized two-phase mixture is used to measure the component fraction with a gamma-ray densitometer

distribution in the tank, we calculated the just suspended impeller speed ( $N_{js}$ ) and obtained the uniform suspended impeller speed by using a speed ratio. The speed was calculated by [19]:

$$N_{js} = Sv^{0.1}[g_c(-\rho_L)/\rho_L]^{0.45}\chi^{0.13}d_p^{0.2}D^{-0.85}, \quad (5)$$

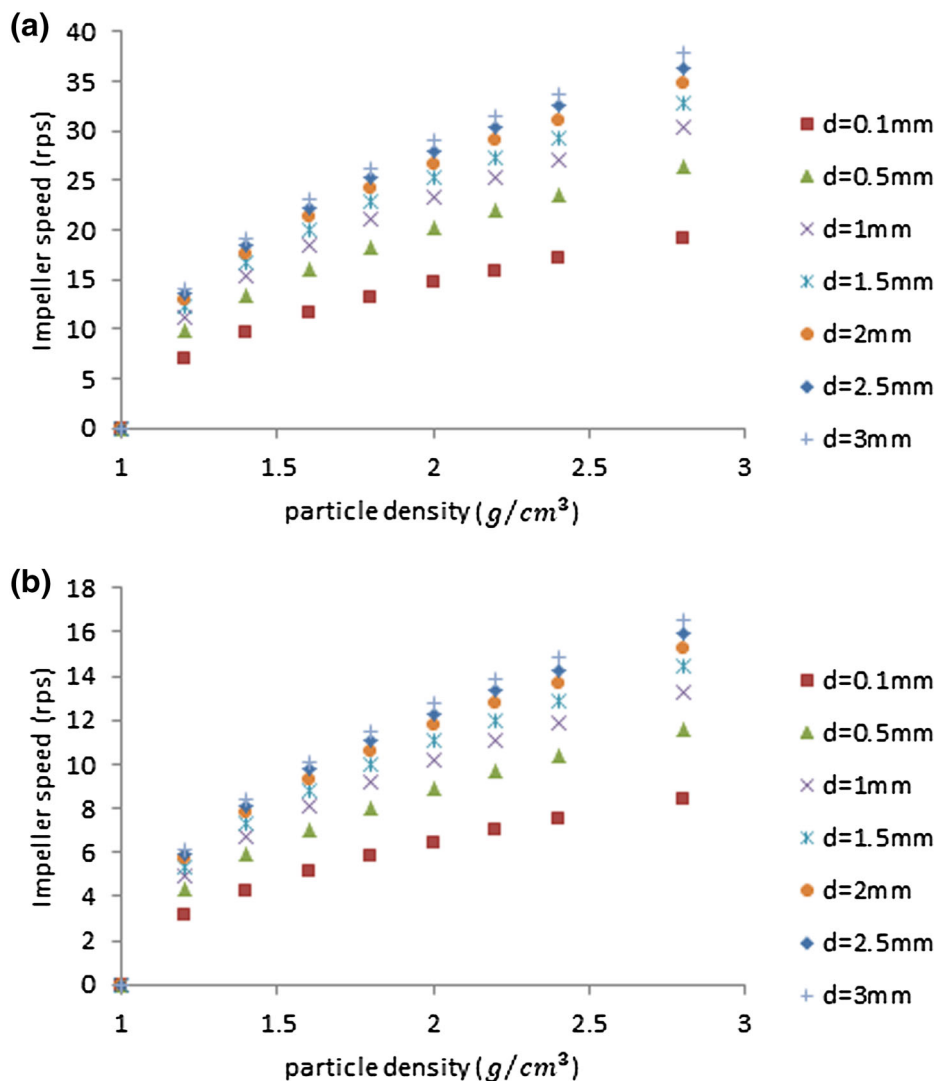
where  $N_{js}$  is in rps;  $S$  is a dimensionless number related to the impeller type, the ratio of impeller diameter to tank diameter, and the ratio of impeller bottom clearance to tank diameter;  $\nu$  is the kinetic viscosity of the liquid ( $m^2/s$ ),  $g_c = 9.81 m^2/s$  the gravitational acceleration constant;  $\rho_S$  is the density of particle ( $kg/m^3$ );  $\rho_L$  is the density of liquid ( $kg/m^3$ );  $\chi$  is the mass ratio of suspended solids to liquid;  $d_p$  is the mass-mean particle diameter (m); and  $D$  is the impeller diameter (m). Assuming, water as the carrier phase,  $S = 4.4$  and a mass ratio equivalent to the maximum permissible solid to liquid mass fraction of unity, using a speed ratio of 1.71, the impeller speed versus the particle density, calculated at different particle sizes, is shown in Fig. 3a. The least-required speed increases with the particle density and size, to achieve a uniform suspended particle-water mixture.

##### 3.1.2 Suspension tank

To achieve a complete off-bottom suspension, calculations were performed on important parameters. To avoid cavitation due to the central interface vortex forms with the commencement of impeller motion and subsequently air bubbles entering the loop, the volume of the tank at a conservative estimate considered to be fourfold the homogenization one. A  $\Phi 10'' \times 30$  cm tank having, with dished bottom, was used. The slurry height to tank diameter ratio was always less than one. We used only one 30° PBT type impeller, with four flat blades of 4 cm width and 2 mm thickness. A complete off-bottom suspension means that no particle remains at the tank bottom for over 1–2 s. The required impeller rotation speed was calculated using Eq. (5), assuming water as the carrier phase,  $S = 7.2$  and a mass ratio of unity. The impeller speed versus the particle density, calculated at different particle sizes, is shown in Fig. 3b. The least-required impeller speed increase with the particle density and size, too, to achieve a complete of bottom suspension. Under the same conditions, it is easier to reach an off-bottom suspension than to reach a homogenization.

By implementing two separate inlets to the two tanks, solid phase was allowed to be slowly added to the liquid one, while circulating the mixture between the two tanks for a better suspension. Figure 4 shows schematically the homogenization and suspension tanks and impellers used in each of them.

**Fig. 3** (Color online) The impeller speed versus particle density at different particle sizes for the homogenization (a) and suspension (b) tanks



3.1.3 Piping, control and drain valves

A closed flow loop was arranged as follows. The outlet nozzle in the bottom of suspension tank is connected to the inlet nozzle in the homogenizer bottom, and the outlet nozzle at the top of homogenizer is connected to the inlet nozzle of suspension tank at the top. This would engage practically all the 16 impellers into the homogenization process, independent of the mass flow rate produced by the pump. An opening delay of a few minutes caused by the control valve installed just below the suspension tank helped a better suspension before the circulation began. After that the mixture was circulated for several minutes, ended by turning off the pump and then closing the second control valve just below the homogenizer tank. While the homogenization mixer was still rotating in an appropriate speed, a homogeneous mixture was sampled for component fraction measurement. A drain valve at the pump outlet

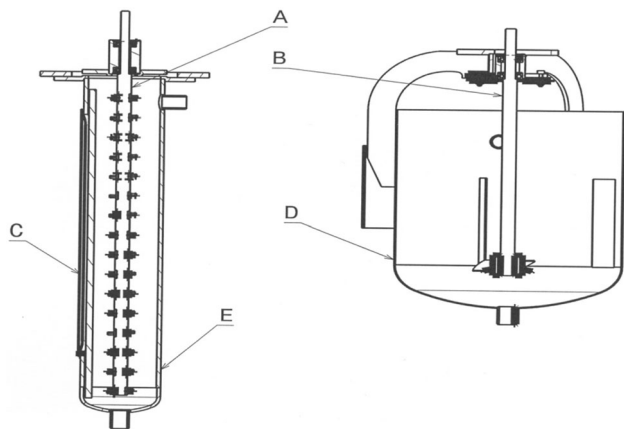


**Fig. 4** Schematic diagrams of the homogenizer and suspension/emulsion tanks

was responsible for slurry discharging after completion of each measurement.

### 3.2 Process set-up

Assuming water as the carrier phase and depending on the particle size and density, the minimum required impeller speed for the suspension and homogenization tanks was extracted from Fig. 3. We set 20 rps as the maximum attainable speed. Otherwise, closing the control valve of suspension tank allowed initially to make an off-bottom suspension, while the impeller was adjusted to the least-required speed and the solid phase was added to the liquid phase step by step. After several minutes, while the control valve of homogenizer tank kept opened, the valve of suspension tank was opened and the pump was turned on immediately. By adjusting impellers of the homogenizer tank to the desired speed to circulate the mixture for a few minutes, the pump and suspension impeller were turned off, and the valve of homogenizer tank was closed. Finally, a uniform suspension was prepared in the homogenizer tank and the component fraction was measured. We note that depending on dispersed phase tendency (to be settled or floated), the impellers should be adjusted to swirl clockwise or vice versa. Depending on the phase volume fractions in each experiment, certain amount of the phase volumes were prepared and fed to the loop. It is easier to prepare a certain mass, instead of volume, in each experiment, using Eq. (6)

$$\beta_S = \alpha_S \rho_S / [\alpha_S \rho_S + \rho_L (1 - \alpha_S)], \quad (6)$$

where  $\beta_S$ ,  $\alpha_S$  and  $\rho_S$  are mass fraction, volume fraction, and density of the solid phase, respectively; and  $\rho_L$  is the liquid phase density. The amount of the solid mass was calculated by

$$m_S = m_L \beta_S / (1 - \beta_S), \quad (7)$$

where  $m_L$  is the mass of liquid phase.

For a suspension, the carrier phase (liquid one) must be entered before the dispersed phase (solid one) is added. For an emulsion, the process is the same but the liquid phase with less density value is considered as the carrier phase.

## 4 Gamma-ray densitometer

In order to confirm performance of homogenization, we used a pre-verified  $\gamma$ -ray densitometer, consisting of a 2 mCi  $^{137}\text{Cs}$  source (at 662 keV, Compton scattering is dominant, and the attenuation coefficient is density-sensitive) a  $2'' \times 2''$  EPIC NaI(Tl) scintillation detector connected to a CR-169 Hamamatsu PMT, the collimators, and the data acquisition system. The electronic modules include the ORTEC 570 amplifier, 550A SCA, and 536

timer/counter. The densitometer was placed on the homogenization tank at a height of 20 cm from the tank bottom. The gamma-ray was collimated into a pencil-beam to pass through the homogeneous mixture and the Plexiglas windows, in thickness of 1 cm, next to the impeller shaft.

### 4.1 Source and detector collimation

The buildup factor is defined as the intensity ratio of the primary and scattered radiations, at any point in a beam, to the intensity of the primary radiation only at that point [20]. Using a pencil-beam detection system with the good geometry conditions, a buildup value of unity can be achieved and component fractions of a homogenized two-phase mixture can be calculated by Eq. 3 or 4. M-C simulations can be done to obtain proper collimators depth and diameter, and to minimum the lead shield volume.

### 4.2 Radiation shielding

The M-C simulations were to calculate lead shielding so that equivalent dose to individuals was below permissible dose limit of radiation workers. ICRP Publication 60 recommended dose limits of an average of 20 mSv per year over 5 years (100 mSv in 5 years) with no more than 50 mSv in a single year [21]. We calculated for a 1 Ci ( $3.7 \times 10^{10}$  Bq)  $^{137}\text{Cs}$  source and a cylindrical lead shield, for the air kerma (kinetic energy released per unit mass) rate at 1 m from the source being no more than 20 mSv/y or 10.42  $\mu\text{Sv/h}$ . All simulations were carried out with the MATLAB-based algorithm [22] and the MCNP code, for a  $^{137}\text{Cs}$  source placed in the center of cylindrical lead shields in height of 10 cm with varying radiuses from 2 to 10 cm. The shield thickness was calculated as follows. Compared to distance where the kerma rate was calculated, the source was small enough in size and could be deemed as a point source. Given a specific gamma-ray emission of  $7.82 \times 10^{-14}$  Sv  $\text{m}^2$  Bq $^{-1}$  h $^{-1}$ , the exposure rate at 1 m from the unshielded source is  $3.7 \times 10^{10}$  Bq  $\times 7.82 \times 10^{-14}$  Sv  $\text{m}^2$  Bq $^{-1}$  h $^{-1}$  /  $1 \text{ m}^2 = 0.0029$  Sv/h.

With a unity buildup factor, using the gamma-ray attenuation coefficient of  $1.24 \text{ cm}^{-1}$  for Pb at 662 keV, the required thickness of lead was calculated at 4.5 cm. Plus one half value layer (HVL) of 0.56 cm for lead at 662 keV, we had the new thickness of 5.06 cm, which is equivalent to  $1.24 \times 5.06 = 6.27$  relaxation length, at which the maximum buildup factor was 1.44, calculated by MATLAB-based algorithm and MCNP. Substituting these values for  $B$  and  $t$  into the Lambert–Beer equation, the  $\gamma$ -ray dose rate was calculate at 7.84  $\mu\text{Sv/h}$ . While the maximum permissible dose rate is 10.42  $\mu\text{Sv/h}$ , the shielding thickness can be 5.06 cm.

**Fig. 5** (Color online) Buildup factor (a) and peripheral to total ratio (b) as a function of the source collimator depth, at various collimator diameters

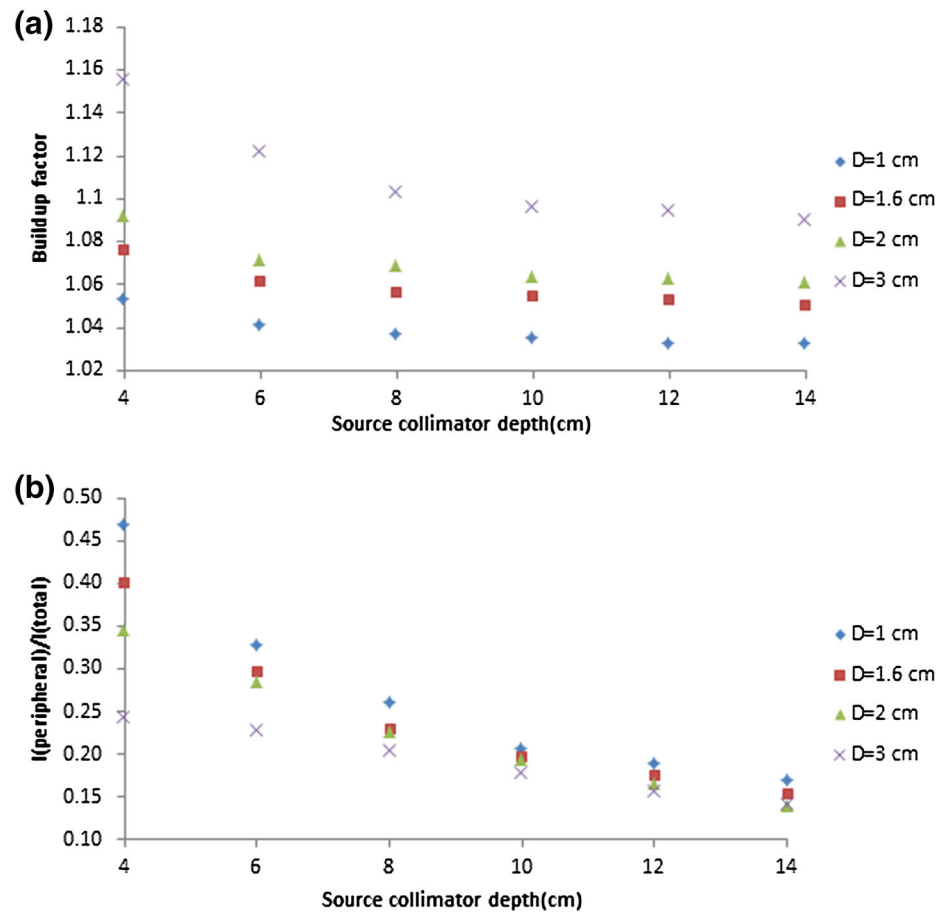


**Table 1** The iron-ore powder desired volume fractions (PVF), the powder mass fraction (PMF) and powder real mass (PRM)

PVF (%)	5	10	15	20	25	30
PMF (%)	16.7	29.7	40.1	48.7	55.9	62.0
PRM (g)	2.40	5.07	8.05	11.40	15.20	19.54

### 4.3 Collimator design

The MATLAB-based algorithm was used to simulate  $^{137}\text{Cs}$  gamma-ray from collimators in depths of 4, 6, 8, 10, 12 and 14 cm and diameters of 1.0, 1.6, 2.0 and 3.0 cm. The detector was placed in a collimator in depth of 4 cm and diameters of 1.0, 1.6, 2.0 and 3.0 cm. The lead cylinders were of 5 cm in wall thickness. All the simulations were done with  $10^8$  particles history and maximum error of  $\pm 1\%$ . The results are shown in Fig. 5a. The buildup factor decreased with increasing source collimator depth, and tended to a constant value after 8 cm, while it increased with the collimator diameter.

It must be noted that, a fraction of radiation can pass through the lead shields without any interaction and entered the peripheral area of the detector. The surface flux crosses the peripheral area of the detector must be

considered as a main source of noise and removed from the transmitted count rate. The noise was defined as the peripheral-to-total ratio and calculated by dividing the transmitted flux at the detector peripheral area to the sum of transmitted fluxes both at the peripheral and central area of the detector. The ratio versus source collimator depth for various diameters is shown in Fig. 5b. The peripheral-to-total flux ratios decreased with increasing source collimator depth and diameter, tended to be equal values for different source diameters after the depth of 8 cm. A greater source collimator diameter means a greater signal-to-noise ratio and accuracy of measurement, subsequently.

## 5 Results

The source collimator used was sized at  $\Phi 1 \text{ cm} \times 8 \text{ cm}$ , and detector was sized at  $\Phi 1 \text{ cm} \times 4 \text{ cm}$ . Different volume fractions (0, 5, 10, 15, 20, 25 and 30%) of iron-ore powder (60% enriched as the dispersed phase) in water (as the carrier phase) were prepared and fed to the homogenizer loop, and measurements were carried out. The homogenizer tank volume was about 3 L, so the carrier

**Table 2** The powder volume fraction (CPVF) calculated at different PPVFs (iron-ore powder prepared volume fractions), averaged count rates (ACR), and correction factors to count rates (CCR) for removing the noise data

PPVF (%)	ACR (counts/s)	CCR (counts/s)	CPVF (%)
0	5893 ± 85	4360 ± 63	0 ± 1.2
5	5145 ± 165	3807 ± 122	5.4 ± 2.2
10	4526 ± 157	3349 ± 116	10.6 ± 2.7
15	4013 ± 142	2970 ± 105	15.4 ± 3.1
20	3535 ± 137	2616 ± 101	20.5 ± 3.6
25	3130 ± 125	2316 ± 93	25.4 ± 4.0
30	2792 ± 106	2066 ± 78	30 ± 4.2

phase (water) initial volume was 12 L. Using Eqs. (6) and (7), by substituting the powder density of 3.8 g/cm<sup>3</sup> and the water density of 1 g/cm<sup>3</sup> the respective mass fraction and real mass to each volume fraction was calculated. Desired powder mass fractions were prepared by adding respective mass fractions to the carrier phase, as is listed in Table 1.

In the calibration stage, the tank filled with just water was counted. Then, corresponding powder mass to the desired volume fraction was added to perform the counting. An experiment was repeated for 10 times, 5 min each. The averaged count rates calculated were corrected by a coefficient of 0.74 to remove the peripheral flux entered the detector, and finally the component fractions was obtained by using Eq. (4). The results are given in Table 2.

## 6 Discussion and conclusion

The results in Table 2, confirm that we have made it possible to measure the component fraction for a two-phase mixture with high density difference between phases.

The attenuation coefficient of each phase is found in calibration stage where the loop is fully filled with water (liquid phase) and partially filled with 30% volume fraction of powder (solid phase).

This laboratory scale test facility is capable of delivering a homogenized suspension and measuring a wide range of two-phase mixtures by the TPFHL loop. In the case of oil–water as an important two-phase mixture, with density difference of 0.15 (while it is 2.8 for the powder–water), by using a speed ratio of 0.27, a uniform mixture could be formed.

The TPFHL can be upgraded to work with mixtures having low density difference between phases, by using a low energy gamma-ray source and reducing the diameter of homogenizer tank, and by new simulations for the gamma-ray source.

**Acknowledgements** The authors wish to thank the fast computing center at the NSTRI due to using the 48-core system to run the Monte Carlo simulations.

## References

- R. Thorn, G.A. Johansen, B.T. Hjertaker, Three-phase flow measurement in the petroleum industry. *Meas. Sci. Technol.* (2013). doi:10.1088/0957-0233/24/1/012003
- American Petroleum Institute, *State of the Art Multiphase Flow Metering API Publication 2566* (API, Washington, 2004)
- S. Corneliussen et al., Handbook of multiphase flow metering, revision 2. *Norwegian Society for Oil and Gas Measurement* (www.nfogn.no)/Tekna (2005)
- <http://cmr.no/facilities/cmr-multiphase-flow-loop/>
- <http://www.prolabnl.com/test-facilities/>
- <http://www.swri.org/4org/d18/mechflu/multflo/fctf/default.htm>
- R. Thorn, G.A. Johansen, E.A. Hammer, Recent developments in three-phase flow measurement. *Meas. Sci. Technol.* (1997). doi:10.1088/0957-0233/8/7/001
- E. Abro, G.A. Johansen, Improved void fraction determination by means of multibeam gamma-ray attenuation measurements. *Flow Meas. Instrum.* (1999). doi:10.1016/S0955-5986(98)00043-0
- S.A. Tjugum, B.T. Hjertaker, G.A. Johansen, Multiphase flow regime identification by multi-beam gamma-ray densitometry. *Meas. Sci. Technol.* (2002). doi:10.1088/0957-0233/13/8/321
- S.A. Tjugum, J. Frieling, G.A. Johansen, A compact low-energy multi beam gamma-ray densitometer for pipe-flow measurements. *Nucl. Instrum. Methods B* (2002). doi:10.1016/S0168-583X(02)01481-7
- I. Ismail, J.C. Gamio, S.F.A. Bukari et al., Tomography for multiphase flow measurement in the oil industry. *Flow Meas. Instrum.* (2005). doi:10.1016/j.flowmeasinst.2005.02.017
- C. Sætre, G.A. Johansen, S.A. Tjugum, Tomographic multiphase flow measurement. *Appl. Radiat. Isot.* (2012). doi:10.1016/j.apradiso.2012.01.022
- M.B. Holstad, G.A. Johansen, S.A. Tjugum, Produced water characterization by dual modality gamma-ray measurements. *Meas. Sci. Technol.* (2005). doi:10.1088/0957-0233/16/4/013
- C.M. Salgado, C. Pereira, R. Schirru et al., Flow regime identification and volume fraction prediction in multiphase flows by means of gamma-ray attenuation and artificial neural networks. *Progr. Nucl. Energy* (2010). doi:10.1016/j.pnucene.2010.02.001
- E. Nazemi, S.A.H. Fegghi, G.H. Roshani, Void fraction prediction in two-phase flows independent of the liquid phase density changes. *Radiat. Meas.* (2014). doi:10.1016/j.radmeas.2014.07.005
- G.H. Roshani, E. Nazemi, S.A.H. Fegghi et al., Flow regime identification and void fraction prediction in two-phase flows based on gamma ray attenuation. *Measurement* (2015). doi:10.1016/j.measurement.2014.11.006
- G.F. Hewitt, P.S. Harrison, S.J. Parry et al., Development and testing of the ‘mixmeter’ multiphase flow meter, in *Proceedings of the 13th North Sea Flow Measurement* (Workshop/ Lillehammer, 1995)
- E.L. Paul, V.A. Atiemo-Obeng, S.M. Kresta, *Handbook of Industrial Mixing: Science and Practice* (Wiley, New York, 2004)
- T.N. Zwietering, Suspending of solid particles in liquid by agitators. *Chem. Eng. Sci.* (1958). doi:10.1016/0009-2509(58)85031-9
- H. Cember, T.E. Johnson, *Introduction to Health Physics*, 4th edn. (McGraw-Hill, New York, 1969)
- ICRP The 2007 Recommendations of ICRP. *Annals of the ICRP* 37(2–4), ICRP Publication 103 2007
- M. Sharifzadeh, H. Afarideh, H. Khalafi et al., A Matlab-based Monte Carlo algorithm for transport of gamma-rays in matter. *Monte Carlo Methods Appl.* (2015). doi:10.1515/mcma-2014-0011